J Exp Biol Advance Online Articles. First posted online on 13 March 2014 as doi:10.1242/jeb.092635
Access the most recent version at http://jeb.biologists.org/lookup/doi/10.1242/jeb.092635

Defective skeletogenesis and oversized otoliths in fish early stages in a changing ocean

Marta S. Pimentel[1,2*], Filipa Faleiro[1], Gisela Dionísio[1,3], Tiago Repolho[1], Pedro Pousão[4], Jorge Machado[2], Rui Rosa[1]

Running head: Fish deformities in a changing ocean

[1] Laboratório Marítimo da Guia, Centro de Oceanografia, Faculdade de Ciências da Universidade de Lisboa, Av. Nossa Senhora do Cabo 939, 2750-374 Cascais, Portugal.
[2] Instituto Ciências Biomédicas Abel Salazar, Universidade do Porto, Largo Prof. Abel Salazar 2, 4099-003 Porto, Portugal.
[3] Departamento de Biologia & CESAM, Universidade de Aveiro, Campus Universitário de Santiago, 3810-193 Aveiro, Portugal
[4] Instituto Português do Mar e da Atmosfera. Av. 5 de Outubro s/n 8700-305, Olhão, Portugal

[*] Corresponding author: Marta Pimentel. Telephone: +351-214869211. Fax: +351-214869720. E-mail: mcrsilva@fc.ul.pt

Keywords: Ocean warming, acidification, fish larvae, ecophysiology, skeletal deformities

Early life stages of many marine organisms are being challenged by rising seawater temperature and CO_2 concentrations, but their physiological responses to these environmental changes still remain unclear. In the present study, we show that future predictions of ocean warming (+4ºC) and acidification (ΔpH = 0.5 units) may compromise the development of early life stages of a highly commercial teleost fish, *Solea senegalensis*. Exposure to future conditions caused a decline in hatching success and larval survival. Growth, metabolic rates and thermal tolerance increased with temperature but decreased under acidified conditions. Hypercapnia and warming amplified the incidence of deformities by 31.5% (including severe deformities such as lordosis, scoliosis and kyphosis), while promoting the occurrence of oversized otoliths (109.3% increase). Smaller larvae with greater skeletal deformities and larger otoliths may face major ecophysiological challenges, which might potentiate substantial declines in adult fish populations, putting in jeopardy the species fitness under a changing ocean.

Introduction

Atmospheric carbon dioxide (CO_2) concentration has increased from pre-industrial levels of 280 µatm to present-day levels of 394 µatm, and it is expected to rise up to 730-1000 µatm by the end of the century (Caldeira and Wickett, 2003; Meehl et al., 2007). Continuous CO_2 uptake by world´s oceans is changing the seawater chemistry and is estimated to lead to a drop of 0.4-0.5 units in seawater pH (Caldeira and Wickett, 2005). Concomitantly, oceans' temperature is rising, and global sea surface temperature is expected to increase approximately 4°C by 2100 (Meehl et al., 2007), leading to profound impacts on marine ecosystems. In fact, the predictable rapid rate of climate change will induce thermal stress to coastal marine biota as their thermal tolerance limits are reached or even exceeded. Beyond a certain thermal limit, biological processes such as metabolism, growth, feeding, reproduction and behavior may be affected (Carmona-Osalde et al., 2004; Portner and Knust, 2007; Nilsson et al., 2009; Byrne, 2011; Pimentel et al., 2012; Rosa et al., 2012), thus compromising the overall fitness and survival of the species. Additionally, under higher temperatures, marine organisms are likely more vulnerable to other environmental stressors such as ocean acidification (Portner, 2008; Byrne et al., 2010; Findlay et al., 2010; Parker et al., 2010; Sheppard Brennand et al., 2010; Byrne, 2011; Rosa et al., 2013; Rosa et al., 2014).

Ocean acidification is considered a major threat to marine organisms as it may lead to acid–base balance disturbances, protein biosynthesis decrease, metabolic depression and growth reduction (Seibel and Walsh, 2001; Portner et al., 2004; Langenbuch et al., 2006; Rosa and Seibel, 2008; Baumann et al., 2012). Exposure to elevated CO_2 particularly affects calcifying organisms (Orr et al., 2005; Dupont et al., 2008; Fabry et al., 2008; Talmage and Gobler, 2010), although detrimental effects on survival, growth and respiratory physiology of non-calcifying marine animals have also been observed (Seibel and Walsh, 2001; Rosa and Seibel, 2008; Munday et al., 2009b).

Fish have developed an effective acid-base regulatory mechanism, which allows them to accumulate bicarbonate and exchange ions across gills under hypercapnic conditions (Portner et al., 2005; Ishimatsu et al., 2008; Melzner et al., 2009). While this is true for adult organisms, early life stages may not benefit from it, as they lack well-developed and specialized ion-regulatory mechanisms to regulate and maintain their internal ionic environment (Morris, 1989; Sayer et al., 1993). Therefore, early life stages are expected to be the most vulnerable to ocean climate change-related conditions and their eventual inability to cope and adapt may constitute a bottleneck for species persistence in a changing ocean (Bauman et al., 2011; Fromell et al., 2012). Until now, only a few studies have scrutinized the impact of ocean climate change on fish larvae performance. While some report negligible effects of ocean acidification on fish larvae (Munday et al. 2011b; Hurst et al., 2012; Harvey et al., 2013; Hurst et al., 2013; Maneja

et al., 2013), others demonstrate that ocean warming and acidification may have a direct impact on embryonic development, larval growth, metabolism, behavior and survival (Bauman et al., 2011; Franke and Clemmesen, 2011; Frommel et al., 2012; Bignami et al., 2013; Pimentel et al., 2014). More recently, it has also been shown that larval otoliths can be affected by changes in the seawater carbonate chemistry (Checkley et al., 2009; Munday et al., 2011a; Bignami et al., 2013), but the impact of hypercapnia on larval fish skeletogenesis still remains unclear.

In the present study, we investigated how the combined effect of warming (+4ºC) and high pCO_2 (0.16% CO_2; pCO_2 = ~1600 µatm; ΔpH = 0.5) affects the hatching success, larval survival, growth, metabolic rates, thermal tolerance limits and skeletogenesis of early life stages of a flatfish, *Solea senegalensis*, with major commercial importance. This teleost fish is an environmentally resilient species that inhabits the Western Iberian Upwelling Ecosystem, the northern limit of the Canary Current Upwelling System, one of the four major eastern boundary currents of the world, where pCO_2 levels may reach up to ~500 µatm (AlvarezSalgado et al., 1997; Perez et al., 1999; Borges and Frankignoulle, 2002). Thus, organisms inhabiting such upwelling ecosystem are commonly exposed to seasonal high pCO_2 events, due to the emergence of deep hypercapnic water masses. In these regions, the future pCO_2 levels are thus expected to exceed the forecasted 1000 µatm for 2100 (Meehl et al., 2007).

Results

Hatching success, larval growth and survival

The impact of high pCO_2 and environmental warming on the hatching success, survival, length and growth of *S. senegalensis* larvae is shown in Figure 1 (see also Supplementary Table 1). Warming had a negative impact on the hatching success of sole larvae ($p<0.05$), but not hypercapnia ($p>0.05$) neither the interaction factor between them ($p>0.05$). The hatching rates decreased from 86.7 ± 5.8% at the present-day scenario to 70.0 ± 10.0% under the future hypercapnic and warming conditions (Fig. 1a).

Survival rates of 30 dph larvae were also significantly affected (Fig. 1b). Both temperature and pCO_2 had a significant effect ($p<0.001$) on survivorship, which decreased from 45.7 ± 1.9% under control conditions to 32.7 ± 2.6% in the future scenario. However, the interaction of both variables was not significant ($p>0.05$). The mean length of 30 dph larvae under control conditions was 13.2 ± 1.5 mm (Fig.1c). Larval growth increased significantly with warming ($p<0.05$), but decreased significantly under acidified conditions ($p<0.05$), with an observed significant interaction effect between these two variables ($p<0.05$). Warming was responsible for increasing length by 48.6 and 46.5% under normocapnic and hypercapnic conditions, respectively. Regardless temperature, *S. senegalensis* larvae became nearly 22% smaller with increasing CO_2. As a result, the highest length value (19.4 ± 1.1 mm) was observed under the

warming and normocapnic scenario, while the lowest length (10.3 ± 0.9 mm) was found at lower temperature and hypercanic conditions. A quite identical trend was observed for SGR, which presented a 23.7-28.4% increase with warming and a 11.9-15.1% decrease with acidification (Fig. 1d). No significant interaction was observed between these two factors ($p>0.05$).

Oxygen consumption rates, thermal sensitivity and thermal tolerance limits

The effect of warming and high pCO_2 on the metabolic rates and thermal tolerance limits of *S. senegalensis* larvae is presented in Figure 2 (see also Supplementary Table 2). Temperature had a positive effect ($p<0.05$) on oxygen consumption rates (OCR), upper thermal tolerance limits (LT50) and critical thermal maximum (CTMax), while hypercapnic conditions promoted a significant reduction ($p<0.05$) on these physiological parameters. Even so, no significant interaction was observed between these two factors ($p>0.05$). OCR of 30 dph larvae increased with temperature from 23.1 ± 3.2 to 34.8 ± 3.5 µmol O_2 $h^{-1}g^{-1}$ and from 16.8 ± 3.8 to 25.3 ± 1.5 µmol O_2 $h^{-1}g^{-1}$ under normocapnic and hypercapnic conditions, respectively (Fig. 2a). These findings represent a decrease of 27.3% under acidified conditions. LT50 of 30 dph larvae increased with temperature from 37.5 ± 0.1 to 37.7 ± 0.0ºC under normocapnia, and from 36.1 ± 0.1 to 38.8 ± 0.3ºC under hypercapnia conditions (Fig. 2b). CTMax of 30 dph larvae followed a similar pattern as for OCR and LT50, increasing with temperature from 37.0 ± 0.9 to 38.3 ± 0.5ºC under normocapnia, and from 35.5 ± 0.6 to 37.3 ± 0.7ºC under hypercapnia conditions (Fig. 2c). Additionally, the development stage had a significant effect ($p<0.05$) over metabolic rates and thermal tolerance limits. *S. senegalensis* hatchlings presented higher OCR and lower LT50 and CTMax values, in comparison to 30 dph larvae (Fig. 2a,b,c).

Thermal sensitivity of *S. senegalensis* larvae between 18ºC and 22ºC ranged between 1.89 and 2.79 (Table 1). Q_{10} values decreased under acidified conditions and increased with fish age.

Skeletal deformities and otolith morphometrics

Several types of skeletal anomalies were found in 30 dph *S. senegalensis* larvae (Table 2; Fig. 3). Skeletal deformities consisted mainly of vertebral abnormalities, such as fusions (Fig. 3c-g), body malformations (Fig. 3c,d), and vertebral curvatures like scoliosis, lordosis and kyphosis (Fig. 3i,j). Structures such as haemal and neural spines and arches were some of the most affected structures across treatments (Fig. 3c-g).

Future ocean warming and high pCO_2 conditions had a significant effect on the incidence of skeletal deformities in *S. senegalensis* larvae (Figs. 4 and 5; see also Supplementary Table 3). Rising temperature and CO_2 levels increased the frequency of total skeletal deformities (Fig. 4a), from 70.9 ± 2.6% at the present-day scenario to 93.2 ± 2.7% under the future conditions ($p<0.05$), an increase of 31.5%. No cranium or pectoral fin deformities were observed under

control temperature and pCO_2 rearing conditions. Under the future scenario, caudal vertebra was the most affected region (Fig. 4d), followed by cranium (Fig. 4b), caudal fin (Fig. 4e), abdominal vertebra (Fig. 4c), pelvic fin (Fig. 4h), dorsal fin (Fig. 4f), and finally the pectoral fins (Fig. 4h). In what concerns severe skeletal deformities, pCO_2 was the main factor contributing to the higher proportion of deformities observed in the future scenario (Fig. 5). Under present-day conditions, less than 1.9% of the larvae presented severe vertebral curvatures such as scoliosis (Fig. 5b) or lordosis (Fig. 5c), and no kyphotic larvae were observed (Fig. 5d). In contrast, all types of severe anomalies significantly increased ($p<0.05$) with future environmental predictions, especially with high pCO_2. The interaction factor between temperature and pCO_2 did not have a significant effect ($p>0.05$) on the incidence of skeletal deformities (including the severe ones), except for abdominal vertebra and dorsal fin deformities.

Otolith size was also greatly affected by future warming and hypercapnia conditions (Fig. 6; see also Supplementary Table 1). *S. senegalensis* larvae experienced a 109.3% increase in otolith area with increasing temperature and pCO_2 ($p<0.05$). Otolith area increased from 1063.6 ± 398.8 mm^2 at the present-day conditions to 1994.5 ± 234.5 mm^2 under warming, and then to 2226.2 ± 187.0 mm^2 under the combined effect of rising temperature and pCO_2. The interaction of both factors was however not significant ($p>0.05$).

Discussion

The future predictions of ocean warming and acidification revealed to have a negative impact on several aspects of the early ontogeny of the environmentally resilient flatfish *S. senegalensis*. Despite the short embryonic development time of this species (less than 2 days), the warming experienced during egg incubation was enough to elicit a negative effect on hatching success. Hatching rates decreased 16.7 percentage points with warming and acidification, in comparison to the present-day conditions. Moreover, the high temperature and pCO_2 levels had a further negative effect on larval survival, representing a decrease of 28.4 percentage points in relation to the present scenario.

As expected, larval growth greatly increased with warming. Increased temperature was responsible for increasing length by 46.5-48.6%. Nevertheless, it is important to keep in mind that this increment does not reflect differences in size at a specific stage of development, as development is accelerated at higher temperatures. In contrast, larval growth decreased under high pCO_2 levels. Contrary to some studies that have shown that larvae can become bigger under high pCO_2 conditions (Munday et al., 2009a; Hurst et al., 2012; Hurst et al., 2013), *S. senegalensis* larvae have become almost 25% smaller with increasing pCO_2.

A quite identical trend was observed for larval metabolic rates and thermal tolerance limits. While temperature had a positive effect on OCR (within normal Q_{10} values) and thermal tolerance limits, hypercapnic conditions triggered a significant reduction on such physiological parameters. Additionally, and as expected, mass-specific metabolic rates decreased with development, while thermal tolerance limits revealed an opposite ontogenetic trend, i.e., older larvae revealed higher thermal tolerance limits than newly-hatched ones. We presume that exposure to higher pCO_2 might have impaired the acid–base balance regulation, which directly affects the efficiency of cellular activities (Portner et al., 2005; Perry and Gilmour, 2006) and may cause deleterious effects on larval physiology and growth.

Faster growth at higher temperatures could have some advantages, since slower growing larvae are potentially more vulnerable to predators and may thus experience greater mortalities (Anderson, 1988). Nevertheless, growth enhancement with temperature might also present some disadvantages, since faster larval growth was accompanied by an increase in the incidence of skeletal deformities. Indeed, temperature is known to be one of the most important environmental factors that can induce morphological deformities during fish development (Aritaki and Seikai, 2004; Georgakopoulou et al., 2010; Dionisio et al., 2012). Additionally, pH may also affect the prevalence of fish skeletal deformities (Lall and Lewis-McCrea, 2007). Although fish skeleton is predominantly composed by calcium phosphate (in the form of hydroxyapatite and cartilaginous material) (Lall and Lewis-McCrea, 2007), additional buffering of tissue pH with bicarbonate and non-bicarbonate ions is expected by acidified conditions, which may interfere with larval skeletal development. In this study, the future warming and high pCO_2 scenario was responsible for increasing the incidence of total skeletal deformities by 22.2 percentage points, affecting 93.1% of the larvae. Moreover, high pCO_2 was the main responsible for the increase of severe skeletal deformities in flatfish larvae. Under the present-day conditions, less than 1.9% of the larvae presented vertebral curvature deformities such as scoliosis or lordosis, and no kyphotic larvae were observed. In contrast, more than 50% of the larvae under the future environmental scenario presented vertebral curvature deformities. These findings are however in disagreement with a recent study that found no effects of CO_2 on the skeletal development of a reef fish (Munday et al., 2011b).

The higher incidence of malformations under the future scenario should however be carefully interpreted. The high percentage of skeletal deformities found in *S. senegalensis* under control temperature and pCO_2 conditions (70.9 ± 2.7%), although similar to the values commonly found for this species under intensive rearing conditions (Fernandez et al., 2009; Dionisio et al., 2012), may indicate that fish were potentially stressed in captivity and would, therefore, be more susceptible to the negative effects of higher temperature and CO_2 levels. Nevertheless, this fact does not exclude the amplifying effect that warming and hypercapnia had on the incidence of skeletal deformities. Even though the increase may be overestimated, the higher rate of

malformations in captive larvae under high temperature and pCO_2 conditions may provide an insight of how future warming and acidification may impact the development of wild flatfish larvae and their future performance in a changing ocean.

Skeletal deformities may impair the ecophysiological performance of fish larvae in many different ways. Vertebral curvatures and fin deformities may affect larval swimming behavior, feeding efficiency and the capacity to maintain their position in a current (Powell et al., 2009). Additionally, larvae with cranium deformities, such as ocular migration anomalies, probably will have their capability to feed, attack prey and avoid predators affected. Larvae with operculum deformities may increase gill's susceptibility to fungus, bacteria and amoebic parasitic infections (Powell et al., 2008) and, as a result, their swimming and cardiovascular performance might be compromised (Powell et al., 2008; Lijalad and Powell, 2009; Powell et al., 2009). Additionally, fish with dental, premaxilar or maxilar deformities cannot adduct their mandible and, besides having potential feeding restrictions, the buccal-opercular pumping of water across gills is also likely to be impaired and compromised (Lijalad and Powell, 2009).

In addition to skeletal deformities, *S. senegalensis* larvae under this future climate change scenario will also be affected by changes in otolith size. *S. senegalensis* larvae experienced a 109.3% increase in otolith area with rising temperature and pCO_2. Although otoliths are calcified structures composed of aragonite-protein bilayers, recent studies revealed that pH regulation in otolith endolymph may lead to increased precipitation of calcium carbonate in otoliths of fingerlings exposed to elevated CO_2 (Checkley et al., 2009; Munday et al. 2011a; Bignami et al., 2013). However, this is not a rule among fishes. In at least one coral reef fish species, otolith size was not affected by exposure to elevated pCO_2 (Munday et al., 2011b). Otoliths are used by fish to sense orientation, acceleration, perception, and to maintain postural equilibrium. Thus, changes in otolith size may have implications for their ecological performance, behavior and individual fitness (Gagliano et al., 2008; Bignami et al., 2013).

In conclusion, the results presented in our study provide a comprehensive insight about the combined effects of ocean warming and hypercapnia conditions on *S. senegalensis* larval development. Fish larval stages represent a critical life phase for species ecological success. Therefore, climate change-related impairments in metabolism, thermal tolerance, growth, skeletal development and survival may lead to substantial declines in adult populations, putting in jeopardy the species persistence under a climate change scenario.

Material and Methods

Egg collection and incubation

S. senegalensis eggs were obtained from a wild-caught broodstock of 4 females and 2 males, under natural spawning conditions at IPMA, Estação Piloto de Piscicultura de Olhão (CRIP Sul,

Olhão, Portugal), during June 2012. After collection, eggs were transported and immediately transferred, under environmental controlled conditions, to the aquaculture facilities in Laboratório Marítimo da Guia (Cascais, Portugal). To estimate the potential physiological responses of early life stages to climate change, *S. senegalensis* eggs and larvae were acclimated for one month at: i) 18ºC - control temperature, the mean sea surface temperature in summer (sSST) and normocapnia (0.04% CO_2; pCO_2 = ~400 µatm); ii) 18ºC and hypercapnia (0.16% CO_2; pCO_2 = ~1600 µatm; ΔpH = 0.5); iii) 22ºC - the future sSST warming scenario for the western coast of Portugal in 2100 (+ 4ºC above the average summer sea surface temperature, Meehl et al., 2007) and normocapnia; and iv) 22ºC and hypercapnia. Prior to releasing the eggs in the rearing tanks, a 2-hour thermal and chemical acclimation was performed.

Eggs and larvae were reared in 12 individual recirculating systems (i.e., 3 systems per treatment), filled with filtered (series of 20, 10, 5 and 0.35 µm) and UV-irradiated natural seawater. Each system comprised a 19 L cylindrical shaped tank (larval rearing tank) connected to a 100 L sump. All rearing tanks were placed inside 400 L water bath tanks (see Supplementary Figure 1), where temperatures (18.0 ± 0.2ºC and 22.0 ± 0.2ºC) were maintained and controlled via seawater chillers (HC-1000A, Hailea, Guangdong, China), in order to ensure thermo-controlled conditions.

Photoperiod was set at 14 L: 10 D (light:dark cycle). Water filtration was performed through mechanical (glass wool), physical (protein skimmer, Schuran, Jülich, Germany) and biological (ouriço® bioballs, Fernando Ribeiro, Portugal) filters, as well as UV sterilization (TMC, Chorleywood, UK). Throughout the experiment, ammonia and nitrite levels were daily monitored and kept below detectable levels. Temperatures were controlled via seawater chillers (Frimar, Fernando Ribeiro, Portugal), while pH was adjusted automatically via a Profilux system (GHL, Kaiserslautern, Germany) connected to pH probes (WaterTech pH 201S) in the rearing tanks and to a standard solenoid valve system connected to a CO_2 tank. Any seawater pH modifications initiated CO_2 addition (if the pH increased) or CO_2 filtered air injection (if the pH decreased), until pH returned to the set value. Additionally, temperature and pH were daily controlled using a digital thermometer (Ebro thermometer TFX430) and a portable pH meter (SevenGo pro™ SG8, Mettler Toledo). Average values were 18.0 ± 0.2ºC and 22.0 ± 0.2ºC for temperature and 8.02 ± 0.05 and 7.51 ± 0.05 for pH. Salinity was kept at 35.4 ± 0.4. Seawater carbonate system speciation (Table 3) was calculated weekly from total alkalinity (determined according to (Sarazin et al., 1999) and pH measurements. Bicarbonate and pCO_2 values were calculated using the CO2SYS program (Lewis and Wallace, 1998), with dissociation constants from (Mehrbach et al., 1973) as refitted by Dickson and Millero (1987).

Larval rearing

Newly-hatched larvae were randomly placed into rearing tanks (19 L volume each), at a stocking density of 70 larvae per liter. All larvae were reared until 30 days post hatching (dph) under the different experimental conditions. Feeding schedule was based on larval development at each experimental condition. Larvae opened the mouth around 2 dph and started to feed on rotifers, *Brachionus plicatilis*, at a density of 5 to 10 rotifer ml^{-1}. Live enriched (AlgaMac-3050) *Artemia* metanauplii were introduced at 5 dph and their proportion was gradually increased from 0.5 to 12 metanauplii ml^{-1}, becoming the only prey offered at 8 dph. Frozen metanauplii were also introduced as feed after larval settlement.

Hatching success, larval growth and survival

The hatching success was analyzed in small rearing boxes placed inside the rearing tanks (one per rearing system). In the beginning of the experiment, a total of 10 eggs (per box) were randomly placed inside each of the 12 boxes (3 per treatment), and were followed throughout the embryonic development. The hatching success was calculated as the percentage of eggs that hatched to normal larvae.

At 0 and 30 dph, 20 larvae per tank (60 larvae per treatment) were randomly sampled and their standard length was measured from the anterior extremity to the urostyle flexion, by means of stereoscopic microscope observations (Leica S6D, Leica Microsystems). The standard length of newly-hatched larvae was 2.57 ± 0.13 mm. The specific embryonic growth rate (SGR) was calculated as:

$$SGR = \frac{(\ln embryo\ size\ (T2) - \ln embryo\ size\ (T1))}{number\ of\ days\ elapsed\ between\ T1\ and\ T2} \times 100.$$

The survival rate was calculated as the percentage of surviving fish by the end of the experiment, with respect to the number of larvae at the beginning of the trial minus those individuals removed for sampling.

Oxygen consumption rates, thermal sensitivity and thermal tolerance limits

Oxygen consumption measurements were determined according to previously established methods (Pimentel et al. 2012; Rosa et al., 2012). Nine newly-hatched (0 dph) and nine 30 dph larvae were incubated at each of the four treatment conditions, in sealed water-jacketed respirometry chambers (RC300 Respiration cell, Strathkelvin Instruments limited, North Lanarkshire, Scotland) containing 0.35-µm filtered and UV-irradiated seawater mixed with antibiotics (50 mg L^{-1} streptomycin), in order to avoid bacterial respiration. Water volumes were adjusted in relation to animal mass (up to 10 mL) in order to minimize locomotion and stress but still allow for spontaneous and routine activity of the hatchlings. Controls (blanks) were used to correct for possible bacterial respiratory activity. Respiration chambers were immersed in water baths (Lauda, Lauda-Königshofen, Germany) to control temperature. Oxygen

concentrations were recorded with Clarke-type O_2 electrodes connected to a multi-channel oxygen interface (Model 928, Strathkelvin Instruments limited, North Lanarkshire, Scotland). The duration of respiratory runs varied between 3 to 6 h. Thermal sensitivity (Q_{10}) was determined using the standard equation:

$$Q_{10} = \frac{R(T2)}{R(T1)}^{\frac{10}{(T2-T1)}},$$

where $R(T_1)$ and $R(T_2)$ represent the oxygen consumption rates at temperatures T_1 and T_2, respectively.

Upper thermal tolerance limits were determined based on previously established methods (Stillman and Somero, 2000). In brief, 0 and 30 dph larvae were incubated in glass containers with approximately 100 mL of 0.35-µm filtered and UV-irradiated seawater collected from the rearing tanks. Each container was stocked with 20 specimens, and a total of 3 containers were used per experimental treatment. These glass containers were suspended in a temperature regulated water bath that was controlled to the nearest 0.1ºC. Water bath temperature was set to the acclimation temperature and maintained for 30 min. Thereafter, temperature was increased at a rate of 1ºC/30 min. Seawater was aerated by means of an air stone and the temperature in each container was checked with thermocouple probes. Every 30 min, if no responsiveness was noticed, the specimen was considered to be dead. The percentage of live individuals at each temperature was calculated, and then transformed by the arcsine square root function and expressed in radians. Linear-regression analysis was then used to find the slope of the line, and the temperature at which 50% of the organisms had died (0.785 radians) was calculated. This was used as a measure of upper thermal tolerance limits and referred to as the LT50. Critical thermal maximum (CTMax) was calculated using the equation:

$$\text{CTMax} = \frac{\Sigma\,\text{T end-point n}}{n},$$

where T end-point is the temperature at which the end-point was reached for individual 1, individual 2, individual n, divided by the n individuals that were in the sample.

Skeletal deformities and otolith morphometrics

To identify and quantify larval skeletal deformities, 20 larvae per rearing tank (60 larvae per treatment) were randomly sampled and fixed in 4% (v/v) buffered paraformaldehyde for 24 h and then transferred to 70% ethanol until double stained. Larvae were stained for bone and cartilage using a modification of the method described by Walker and Kimmel (2007), and observed under a stereoscopic microscope (Leica S6D, Leica Microsystems), in order to identify skeletal deformities. Skeletal deformities were defined according to previously established methods (Wagemans et al., 1998; Gavaia et al., 2002; Deschamps et al., 2008; Fernandez et al., 2009; Dionisio et al., 2012). Deformities were divided into several categories according to the affected structure (e.g., cranium, abdominal vertebra, caudal vertebra, caudal fin, dorsal fin,

pectoral fin and pelvic fin), and are described in Table 2. Skeletal deformities such as scoliosis, lordosis, kyphosis, multiple vertebral fusions or more than three anomalies per individual were considered severe deformities. Skeletal deformities were quantified as the percentage of fish exhibiting a specific deformity.

In order to analyze otolith area, 20 larvae per rearing tank (60 larvae per treatment) were randomly selected, measured and preserved in absolute ethanol. The left and right sagittal otoliths of each individual were removed and photographed under a stereoscopic microscope (Leica S6D, Leica Microsystems). Otolith area was measured using the ImageJ program©. Otolith area was calculated as the mean of the right and left otoliths, and normalized to fish length.

Statistical analysis

ANOVA was used to test for significant differences between the tanks of each experimental treatment. Since no differences were found between tanks, all the samples from the same treatment were pooled and analyzed together. Two-way ANOVA were then conducted in order to detect significant differences in hatching success, larval survival, standard length, SGR, skeletal deformities and otolith size between temperature and pCO_2 treatments. Three-way ANOVA were applied to detect significant differences in OCR, LT50 and CTMax between temperature and pCO_2 treatments and development stage (0 and 30 dph). Subsequently, post-hoc Tukey HSD tests were performed. All statistical analyses were performed for a significance level of 0.05, using Statistica 10.0 software (StatSoft Inc., Tulsa, USA).

Acknowledgements

We would like to thank CRIP Sul for supplying fish eggs, and to Oceanário de Lisboa and Aquário Vasco da Gama for supplying rotifers and microalgae. We also thank Lloyd Trueblood for helpful suggestions and critically reviewing the manuscript. The Portuguese Foundation for Science and Technology (FCT) supported this study through doctoral grants to MSP (SFRH/BD/81928/2011) and GD (SFRH/BD/73205/2010), a post-doc grant (SFRH/BPD/79038/2011) to FF and project grant to RR (PTDC/AAG-GLO/3342/2012).

Author contributions

R.R. designed the experiment; M.S.P. and F.F. performed the experiment; M.S.P., F.F., G.D., T.R., P.P., J.M. and R.R. analyzed data; M.S.P., F.F. and R.R. wrote the main paper. All authors discussed the results and their implications, and commented on the manuscript at all stages.

References

AlvarezSalgado, X. A., Castro, C. G., Perez, F. F. and Fraga, F. (1997). Nutrient mineralization patterns in shelf waters of the Western Iberian upwelling. *Cont. Shelf Res.* **17**, 1247-1270.

Anderson, J. T. (1988). A review of size dependent survival during pre-recruit stages of fishes in relation to recruitment. *J. Northw. Atl. Fish. Sci.* **8**, 55-56.

Aritaki, M. and Seikai, T. (2004). Temperature effects on early development and occurrence of metamorphosis-related morphological abnormalities in hatchery-reared brown sole Pseudopleuronectes herzensteini. *Aquaculture* **240**, 517-530.

Baumann, H., Talmage, S. C. and Gobler, C. J. (2012). Reduced early life growth and survival in a fish in direct response to increased carbon dioxide. *Nature Clim. Change* **2**, 38-41.

Bignami, S., Sponaugle, S. and Cowen, R. K. (2013). Response to ocean acidification in larvae of a large tropical marine fish, Rachycentron canadum. *Glob. Change Biol.* **19**, 996-1006.

Borges, A. V. and Frankignoulle, M. (2002). Distribution of surface carbon dioxide and air-sea exchange in the upwelling system off the Galician coast. *Global Biogeochem. CY.* **16**.

Byrne, M. (2011). Impact of ocean warming and ocean acidification on marine invertebrate life history stages: vulnerability and potential for persistence in a changing ocean. *Oceanogr. Mar. Biol.* **49**, 1-42.

Byrne, M., Soars, N., Selvakumaraswamy, P., Dworjanyn, S. A. and Davis, A. R. (2010). Sea urchin fertilization in a warm, acidified and high pCO(2) ocean across a range of sperm densities. *Mar. Environ. Res.* **69**, 234-239.

Caldeira, K. and Wickett, M. E. (2003). Anthropogenic carbon and ocean pH. *Nature* **425**, 365-365.

Caldeira, K. and Wickett, M. E. (2005). Ocean model predictions of chemistry changes from carbon dioxide emissions to the atmosphere and ocean. *J. Geophys. Res.* **110**.

Carmona-Osalde, C., Rodriguez-Serna, M., Olvera-Novoa, M. A. and Gutierrez-Yurrita, P. J. (2004). Gonadal development, spawning, growth and survival of the crayfish Procambarus llamasi at three different water temperatures. *Aquaculture* **232**, 305-316.

Checkley, D. M., Dickson, A. G., Takahashi, M., Radich, J. A., Eisenkolb, N. and Asch, R. (2009). Elevated CO2 Enhances Otolith Growth in Young Fish. *Science* **324**, 1683-1683.

Deschamps, M. H., Kacem, A., Ventura, R., Courty, G., Haffray, P., Meunier, F. J. and Sire, J. Y. (2008). Assessment of "discreet" vertebral abnormalities, bone mineralization and bone compactness in farmed rainbow trout. *Aquaculture* **279**, 11-17.

Dickson, A. and Millero, F. (1987). A comparison of the equilibrium constants for the dissociation of carbonic acid in seawater media. . *Deep-Sea Res.* **34**, 1733-1743.

Dionisio, G., Campos, C., Valente, L. M. P., Conceicao, L. E. C., Cancela, M. L. and Gavaia, P. J. (2012). Effect of egg incubation temperature on the occurrence of skeletal deformities in Solea senegalensis. *J. Appl. Ichthyol.* **28**, 471-476.

Dupont, S., Havenhand, J., Thorndyke, W., Peck, L. and Thorndyke, M. (2008). Near-future level of CO2-driven ocean acidification radically affects larval survival and development in the brittlestar Ophiothrix fragilis. *Mar. Ecol. Prog. Ser.* **373**, 285-294.

Fabry, V. J., Seibel, B. A., Feely, R. A. and Orr, J. C. (2008). Impacts of ocean acidification on marine fauna and ecosystem processes. *Ices Mar. Res.* **65**, 414-432.

Fernandez, I., Pimentel, M. S., Ortiz-Delgado, J. B., Hontoria, F., Sarasquete, C., Estevez, A., Zambonino-Infante, J. L. and Gisbert, E. (2009). Effect of dietary vitamin A on Senegalese sole (Solea senegalensis) skeletogenesis and larval quality. *Aquaculture* **295**, 250-265.

Findlay, H. S., Kendall, M. A., Spicer, J. I. and Widdicombe, S. (2010). Relative influences of ocean acidification and temperature on intertidal barnacle post-larvae at the northern edge of their geographic distribution. *Estuar. Coast. Shelf S.* **86**, 675-682.

Franke, A. and Clemmesen, C. (2011). Effect of ocean acidification on early life stages of Atlantic herring (Clupea harengus L.). *Biogeosciences Discuss.* **8**, 3697-3707.

Frommel, A. Y., Maneja, R., Lowe, D., Malzahn, A. M., Geffen, A. J., Folkvord, A., Piatkowski, U., Reusch, T. B. H. and Clemmesen, C. (2012). Severe tissue damage in Atlantic cod larvae under increasing ocean acidification. *Nature clim. Change* **2**, 42-46.

Gagliano, M., Depczynski, M., Simpson, S. D. and Moore, J. A. Y. (2008). Dispersal without errors: symmetrical ears tune into the right frequency for survival. *Proc. R. Soc. Lond. B Biol. Sci.* **275**, 527-534.

Gavaia, P. J., Dinis, M. T. and Cancela, M. L. (2002). Osteological development and abnormalities of the vertebral column and caudal skeleton in larval and juvenile stages of hatchery-reared Senegal sole (Solea senegalensis). *Aquaculture* **211**, 305-323.

Georgakopoulou, E., Katharios, P., Divanach, P. and Koumoundouros, G. (2010). Effect of temperature on the development of skeletal deformities in Gilthead seabream (Sparus aurata Linnaeus, 1758). *Aquaculture* **308**, 13-19.

Harvey, B. P., Gwynn-Jones, D. and Moore, P. J. (2013). Meta-analysis reveals complex marine biological responses to the interactive effects of ocean acidification and warming. *Ecol. Evol.* **3**, 1016-1030.

Hurst, T. P., Fernandez, E. R. and Mathis, J. T. (2013). Effects of ocean acidification on hatch size and larval growth of walleye pollock (Theragra chalcogramma). *Ices J. Mar. Sci.* **70**, 812-822.

Hurst, T. P., Fernandez, E. R., Mathis, J. T., Miller, J. A., Stinson, C. M. and Ahgeak, E. F. (2012). Resiliency of juvenile walleye pollock to projected levels of ocean acidification. *Aquatic Biol.* **17**, 247-259.

Ishimatsu, A., Hayashi, M. and Kikkawa, T. (2008). Fishes in high-CO2, acidified oceans. *Mar. Ecol. Prog. Ser.* **373**, 295-302.

Langenbuch, M., Bock, C., Leibfritz, D. and Portner, H. O. (2006). Effects of environmental hypercapnia on animal physiology: A C-13 NMR study of protein synthesis rates in the marine invertebrate Sipunculus nudus. *Comp. Biochem. Physiol. A Mol. Integr. Physiol.* **144**, 479-484.

Lewis, E. and Wallace, D. W. R. (1998). CO2SYS-Program developed for the CO2 system calculations. *Carbon Dioxide Inf Anal Center, Report ORNL/CDIAC-105*.

Lijalad, M. and Powell, M. D. (2009). Effects of lower jaw deformity on swimming performance and recovery from exhaustive exercise in triploid and diploid Atlantic salmon Salmo salar L. *Aquaculture* **290**, 145-154.

Maneja, R. H., Frommel, A. Y., Geffen, A. J., Folkvord, A., Piatkowski, U., Chang, M. Y. and Clemmesen, C. (2013). Effects of ocean acidification on the calcification of otoliths of larval Atlantic cod Gadus morhua. *Mar. Ecol. Progr. Ser.* **477**, 251-258.

Meehl, G. A., Stocker, T. F., Collins, W. D., Friedlingstein, P., Gaye, A. T., Gregory, J. M., Kitoh, A., Knutti, R., Murphy, J. M., Noda, A. et al. (2007). Climate Change 2007: The Physical Science Basis. Contribution of Working Group I to the Fourth Assessment Report of the Intergovernmental Panel on Climate Change. Cambridge, United Kingdom: Cambridge University Press.

Mehrbach, C., Culberson, C., Hawley, J. and Pytkowicz, R. (1973). Measurement of the apparent dissociation constants of carbonic acid in seawater at atmospheric pressure. *Limnol. Oceanogr* **18**, 897-907.

Melzner, F., Gutowska, M. A., Langenbuch, M., Dupont, S., Lucassen, M., Thorndyke, M. C., Bleich, M. and Portner, H. O. (2009). Physiological basis for high CO2 tolerance in marine ectothermic animals: pre-adaptation through lifestyle and ontogeny? *Biogeosciences* **6**, 2313-2331.

Morris, R. (1989). Acid Toxicity and Aquatic Animals. Cambridge, United Kingdom: Cambridge University.

Munday, P. L., Donelson, J. M., Dixson, D. L. and Endo, G. G. K. (2009a). Effects of ocean acidification on the early life history of a tropical marine fish. *Proc. R. Soc. B.* **276**, 3275-3283.

Munday, P. L., Hernaman, V., Dixson, D. L. and Thorrold, S. R. (2011a). Effect of ocean acidification on otolith development in larvae of a tropical marine fish. *Biogeosciences* **8**, 1631-1641.

Munday, P. L., Gagliano, M., Donelson, J. M., Dixson, D. L. and Thorrold, S. R. (2011b). Ocean acidification does not affect the early life history development of a tropical marine fish. *Mar. Ecol. Prog. Ser.* **423**, 211-221.

Munday, P. L., Dixson, D. L., Donelson, J. M., Jones, G. P., Pratchett, M. S., Devitsina, G. V. and Doving, K. B. (2009b). Ocean acidification impairs olfactory discrimination and homing ability of a marine fish. *Proc. Nat. Acad. Sci. U.S.A.* **106**, 1848-1852.

Nilsson, G. E., Crawley, N., Lunde, I. G. and Munday, P. L. (2009). Elevated temperature reduces the respiratory scope of coral reef fishes. *Glob. Change Biol.* **15**, 1405-1412.

Orr, J. C., Fabry, V. J., Aumont, O., Bopp, L., Doney, S. C., Feely, R. A., Gnanadesikan, A., Gruber, N., Ishida, A., Joos, F. et al. (2005). Anthropogenic ocean acidification over the twenty-first century and its impact on calcifying organisms. *Nature* **437**, 681-686.

Parker, L. M., Ross, P. M. and O'Connor, W. A. (2010). Comparing the effect of elevated pCO(2) and temperature on the fertilization and early development of two species of oysters. *Mar. Biol.* **157**, 2435-2452.

Perez, F. F., Rios, A. F. and Roson, G. (1999). Sea surface carbon dioxide off the Iberian Peninsula (North Eastern Atlantic Ocean). *J. Marine Syst.* **19**, 27-46.

Perry, S. F. and Gilmour, K. M. (2006). Acid-base balance and CO2 excretion in fish: Unanswered questions and emerging models. *Respir. Physiol. Neurobiol.* **154**, 199-215.

Pimentel, M., Pregado, M., Repolho, T. and Rosa, R. (2014). Impact of ocean acidification in the metabolism and swimming behavior of the dolphinfish (Coryphaena hippurus) early larvae. *Mar. Biol.* **161**, 725-729.

Pimentel, M. S., Trubenbach, K., Faleiro, F., Boavida-Portugal, J., Repolho, T. and Rosa, R. (2012). Impact of ocean warming on the early ontogeny of cephalopods: a metabolic approach. *Mar. Biol.* **159**, 2051-2059.

Portner, H. O. (2008). Ecosystem effects of ocean acidification in times of ocean warming: a physiologist's view. *Mar. Ecol. Prog.* **373**, 203-217.

Portner, H. O. and Knust, R. (2007). Climate change affects marine fishes through the oxygen limitation of thermal tolerance. *Science* **315**, 95-97.

Portner, H. O., Langenbuch, M. and Reipschlager, A. (2004). Biological impact of elevated ocean CO2 concentrations: Lessons from animal physiology and earth history. *J. Ocean.* **60**, 705-718.

Portner, H. O., Langenbuch, M. and Michaelidis, B. (2005). Synergistic effects of temperature extremes, hypoxia, and increases in CO2 on marine animals: From Earth history to global change. *J. Geophys. Res. Oceans.* **110**.

Powell, M. D., Jones, M. A. and Lijalad, M. (2009). Effects of skeletal deformities on swimming performance and recovery from exhaustive exercise in triploid Atlantic salmon. *Dis. Aquat. Org.* **85**, 59-66.

Powell, M. D., Leef, M. J., Roberts, S. D. and Jonesk, M. A. (2008). Neoparamoebic gill infections: host response and physiology in salmonids. *J. Fish. Biol.* **73**, 2161-2183.

Rosa, R. and Seibel, B. A. (2008). Synergistic effects of climate-related variables suggest future physiological impairment in a top oceanic predator. *Proc. Natl. Acad. Sci. USA.* **105**, 20776-20780.

Rosa, R., Pimentel, M. S., Boavida-Portugal, J., Teixeira, T., Trubenbach, K. and Diniz, M. (2012). Ocean Warming Enhances Malformations, Premature Hatching, Metabolic Suppression and Oxidative Stress in the Early Life Stages of a Keystone Squid. *Plos One* **7**.

Rosa, R., Trübenbach, K., Pimentel, M. S., Boavida-Portugal, J., Faleiro, F., Baptista, M., Dionísio, G., Calado, R., Pörtner, H. O. and Repolho, T. (2014). Differential impacts of ocean acidification and warming on winter and summer progeny of a coastal squid (Loligo vulgaris). *J. Exp. Biol.* **217**, 518-525.

Rosa, R., Trübenbach, K., Repolho, T., Pimentel, M., Faleiro, F., Boavida-Portugal, J., Baptista, M., Lopes, V. M., Dionísio, G., Leal, M. et al. (2013). Lower hypoxia thresholds of cuttlefish early life stages living in a warm acidified ocean. *Proc. R. Soc. B.* **280**.

Sarazin, G., Michard, G. and Prevot, F. (1999). A rapid and accurate spectroscopic method for alkalinity measurements in sea water samples. *Water Res.* **33**, 290-294.

Sayer, M. D. J., Reader, J. P. and Dalziel, T. R. K. (1993). Fresh-water acidification effects on the early-life stages of fish. Rev. Fish Biol. Fish. **3**, 95-132.
Seibel, B. A. and Walsh, P. J. (2001). Carbon cycle - Potential, impacts of CO2 injection on deep-sea biota. *Science* **294**, 319-320.
Sheppard Brennand, H., Soars, N., Dworjanyn, S. A., Davis, A. R. and Byrne, M. (2010). Impact of Ocean Warming and Ocean Acidification on Larval Development and Calcification in the Sea Urchin Tripneustes gratilla. *Plos One* **5**.
Stillman, J. H. and Somero, G. N. (2000). A comparative analysis of the upper thermal tolerance limits of eastern Pacific porcelain crabs, genus Petrolisthes: Influences of latitude, vertical zonation, acclimation, and phylogeny. *Physiol. Biochem. Zool.* **73**, 200-208.
Talmage, S. C. and Gobler, C. J. (2010). Effects of past, present, and future ocean carbon dioxide concentrations on the growth and survival of larval shellfish. *Proc. Natl Acad. Sci. USA.* **107**, 17246-17251.
Wagemans, F., Focant, B. and Vandewalle, P. (1998). Early development of the cephalic skeleton in the turbot. *J. Fish Biol.* **52**, 166–204.

Table 1 - Thermal sensitivity (Q_{10}) between 18 and 22ºC of 0 and 30 dph *Solea senegalensis* larvae at normo- and hypercapnia.

Development stage	pH	Q_{10}
0 dph	7.5	1.89
	8.0	2.62
30 dph	7.5	2.77
	8.0	2.79

624 **Table 2 - Types of skeletal deformities considered in this study** (adapted from Wagemans et
625 al., 1998; Gavaia et al., 2002; Dionísio et al., 2012).
626

Affected area	Types of skeletal deformiies	Description
Cranium	Jaw deformities	Malformed and/or reduced maxillary, premaxillary, angular and/or dentary bones
	Ocular migration deformities	Incomplete or non-existent ocular migration
	Deformed opercle	Deformed opercular, ceratobranchial and ceratohyal bones
Abdominal vertebra	Vertebral body malformation	Torsion and/or malformation of one or more vertebrae
	Vertebral fusion	Partial or total fusion of two or more vertebrae
	Vertebral compression	Partial or total compression of two or more vertebrae
	Malformed neural and/or haemal arch	Deformed, absent or fused
	Malformed neural and/or haemal spine	Deformed, absent or fused
	Malformed parapophysis	Deformed, absent, fused or supernumerary
	Scoliosis	Side-to-side vertebral curvature
	Lordosis	Excessive inward vertebral curvature
	Kyphosis	Excessive outward vertebral curvature
Caudal vertebra	Vertebral body malformation	Torsion and/or malformation of one or more vertebrae
	Vertebral fusion	Partial or total fusion of two or more vertebrae
	Vertebral compression	Partial or total compression of two or more vertebrae
	Malformed neural and/or haemal arch	Deformed, absent, asymmetric or fused
	Malformed neural and/or haemal spine	Deformed, absent, asymmetric or fused
	Scoliosis	Side-to-side vertebral curvature
	Lordosis	Excessive inward vertebral curvature
Caudal fin complex	Malformed hypural	Deformed, absent, asymmetric, fused or supernumerary
	Malformed epural	Deformed, absent, asymmetric, fused or supernumerary
	Malformed parahypural	Deformed, absent, asymmetric, fused or supernumerary
	Malformed fin rays	Deformed, absent, asymmetric, fused or supernumerary
Dorsal fin	Malformed fin rays	Deformed, absent, asymmetric, fused or supernumerary
	Malformed pterygiophores	Deformed, absent, fused or supernumerary
Pectoral/pelvic fin	Malformed fin rays	Deformed, absent, asymmetric, fused or supernumerary

627
628
629
630
631

Table 3 - Seawater carbonate chemistry data for the different climate change scenarios. Total carbon (C_T), carbon dioxide partial pressure (pCO_2), bicarbonate concentration (HCO_3^-) and aragonite saturation state of seawater (Ω_{arag}) were calculated with CO2SYS using salinity, temperature, pH and total alkalinity (A_T). Values are means ± SD.

Temperature (ºC)	pH (Total scale)	A_T [µmol kg^{-1}SW]	C_T [µmol/kg^{-1} SW]	pCO_2 [µatm]	HCO_3^- [µmol kg^{-1}]	Ω_{arag}
22.02 ± 0.42	8.03 ± 0.05	2335.74 ± 89.09	2148.20 ± 81.43	424.53 ± 19.97	1985.25 ± 75.28	2.24 ± 0.08
22.12 ± 1.01	7.51 ± 0.05	2317.40 ± 36.40	2314.73 ± 36.72	1654.20 ± 49.06	2194.88 ± 34.84	0.78 ± 0.01
18.20 ± 0.40	8.02 ± 0.04	2305.70 ± 80.54	2141.80 ± 76.78	400.00 ± 66.71	1993.35 ± 72.21	1.95 ± 0.07
18.15 ± 0.29	7.50 ± 0.03	2281.07 ± 61.89	2290.90 ± 62.73	1607.90 ± 24.78	2173.55 ± 59.50	0.67 ± 0.02

Figure captions

Figure 1 - Effect of ocean warming and acidification on the early stages of *Solea senegalensis*. Hatching success (n=30) (**a**) and survival rate (n=3) (**b**), standard length (n=60) (**c**) and specific growth rate (SGR) (n=60) (**d**) of 30 dph larvae at different temperature and pH scenarios. Values are given in mean ± SD. Different letters represent significant differences between the different climate scenarios ($p<0.05$) (more statistical details in Supplementary Table 1).

Figure 2 - Impact of ocean warming and acidification on the metabolism and thermal tolerance of *Solea senegalensis* larvae. Oxygen consumption rates (OCR) (n=9) (**a**), upper thermal tolerance limits (LT50) (n=30) (**b**), and critical thermal maximum (CTMax) (n=30) (**c**) of 0 and 30 dph larvae (dark and light grey, respectively) at different temperature and pH scenarios. Values are given in mean ± SD. Different letters represent significant differences between the different climate scenarios ($p<0.05$). Asterisks represent significant differences between the two developmental stages ($p<0.05$) (more statistical details in Supplementary Table 2).

Figure 3 - Skeletal deformities of 30 dph *Solea senegalensis* larvae under the effect of ocean warming and acidification. Cranium deformity, ocular migration anomaly (**a**); opercle and cranium deformity (**b**); vertebra fusion and compression, deformed spines, arches and parapophysis (**c**); vertebra fusion and deformed spines and arches (**d**); vertebra fusion, urostyle fusion and caudal fin complex anomalies such as modified neural and hemal spine, hypural and fin rays (**e**); vertebra fusion and compression, deformed spines and arches (**f**); vertebral fusion, deformed hypural and modified hemal spines (**g**); pelvin fin deformity (**h**); scoliosis (**i**); lordosis and kyphosis (**j**).

Figure 4 - Incidence of skeletal deformities in *Solea senegalensis* larvae under the effect of ocean warming and acidification. Total skeletal deformities of 30 dph larvae at different temperature and pH scenarios (**a**), which include deformities in the cranium (**b**), abdominal vertebra (**c**), caudal vertebra (**d**), caudal fin complex (**e**), dorsal fin (**f**), pectoral fin (**g**), and pelvic fin (**h**). Values are given in mean ± SD (n=60). Different letters represent significant differences between the different climate scenarios ($p<0.05$) (more statistical details in Supplementary Table 3).

Figure 5 - Incidence of severe skeletal deformities in *Solea senegalensis* larvae under the effect of ocean warming and acidification. Total severe skeletal deformities (**a**) and severe

vertebral curvatures such as lordosis (**b**), scoliosis (**c**), and kyphosis (**d**) of 30 dph larvae at different temperature and pH scenarios. Values are given in mean ± SD (n=60). Different letters represent significant differences between the different climate scenarios ($p<0.05$) (more statistical details in Supplementary Table 3).

Figure 6 - Effect of ocean warming and acidification on otolith size of 30 dph *Solea senegalensis* larvae. Otolith area at different temperature and pH scenarios. Values are given in mean ± SD (n=60). Different letters represent significant differences between the different climate scenarios ($p<0.05$) (more statistical details in Supplementary Table 1).

Figure 1

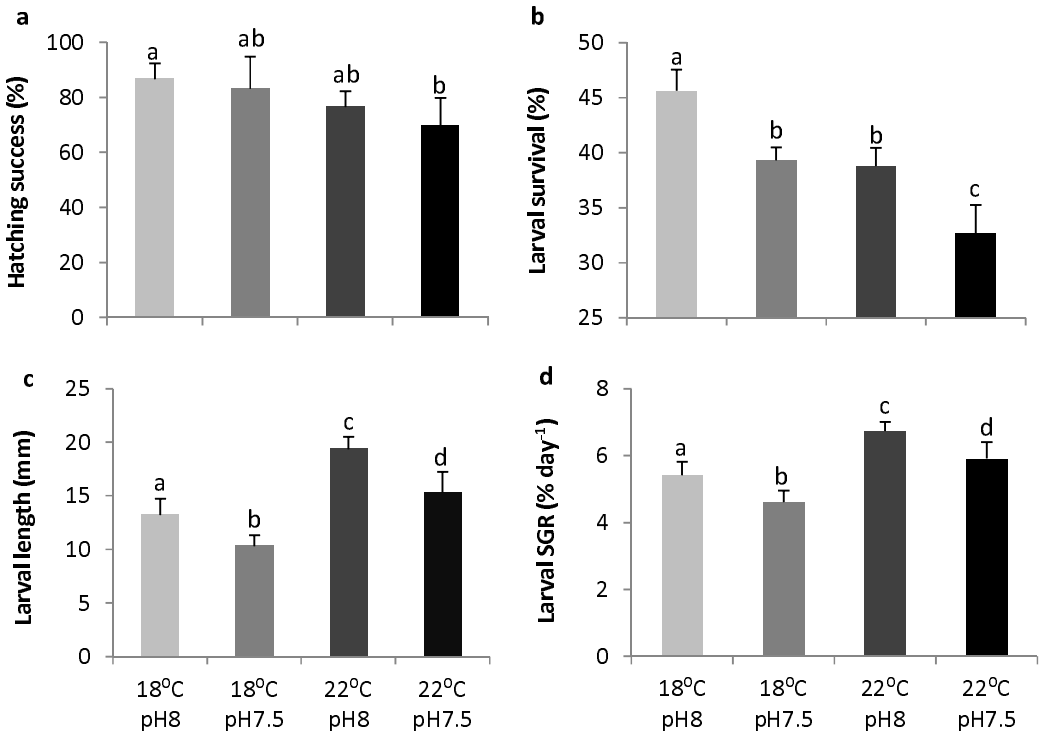

Figure 2

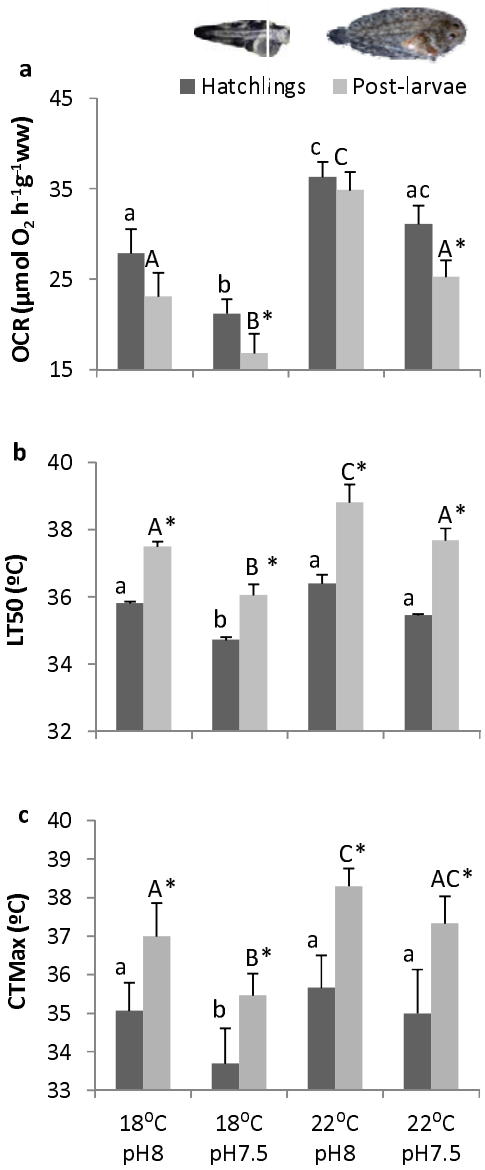

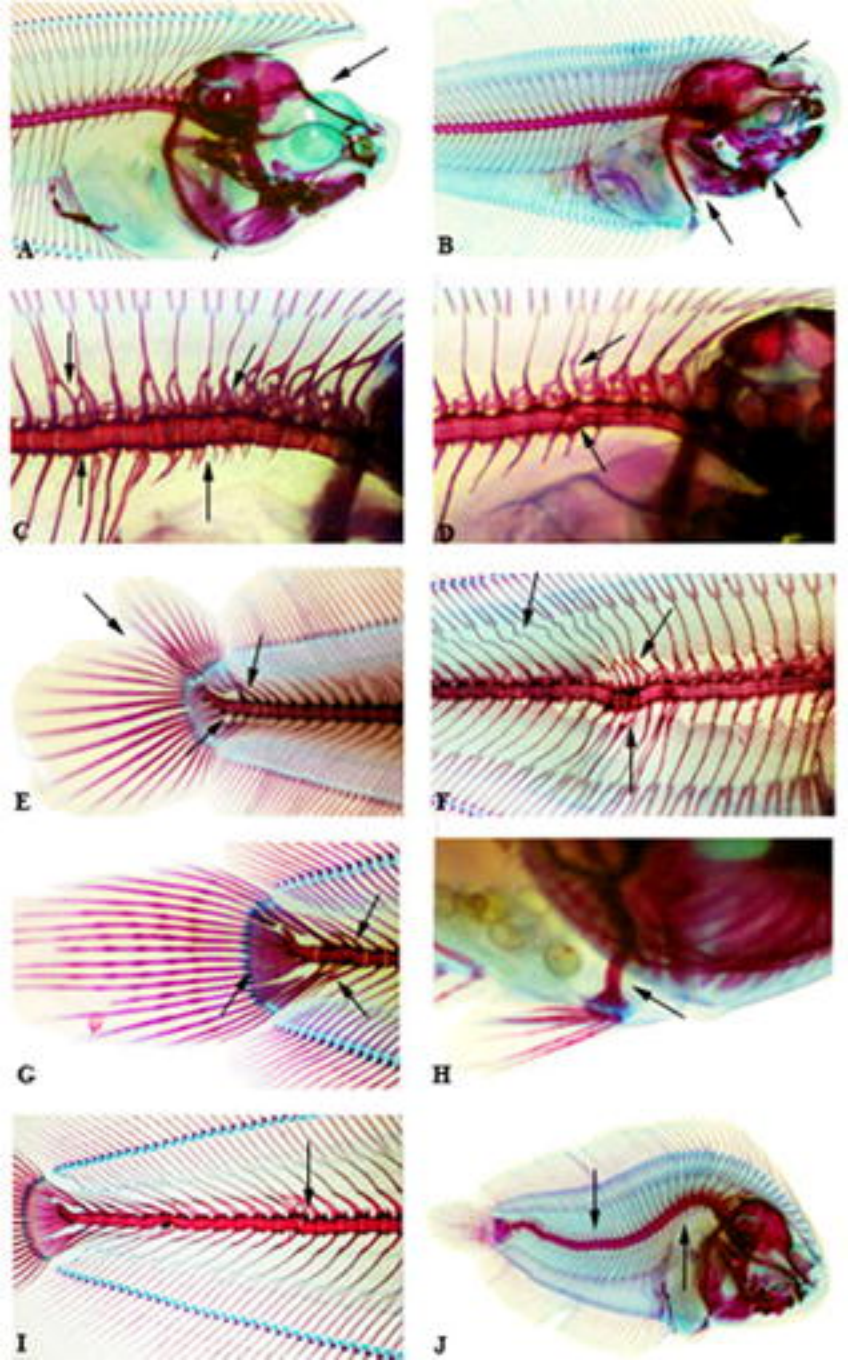
A
B
C
D
E
F
G
H
I
J

Figure 4

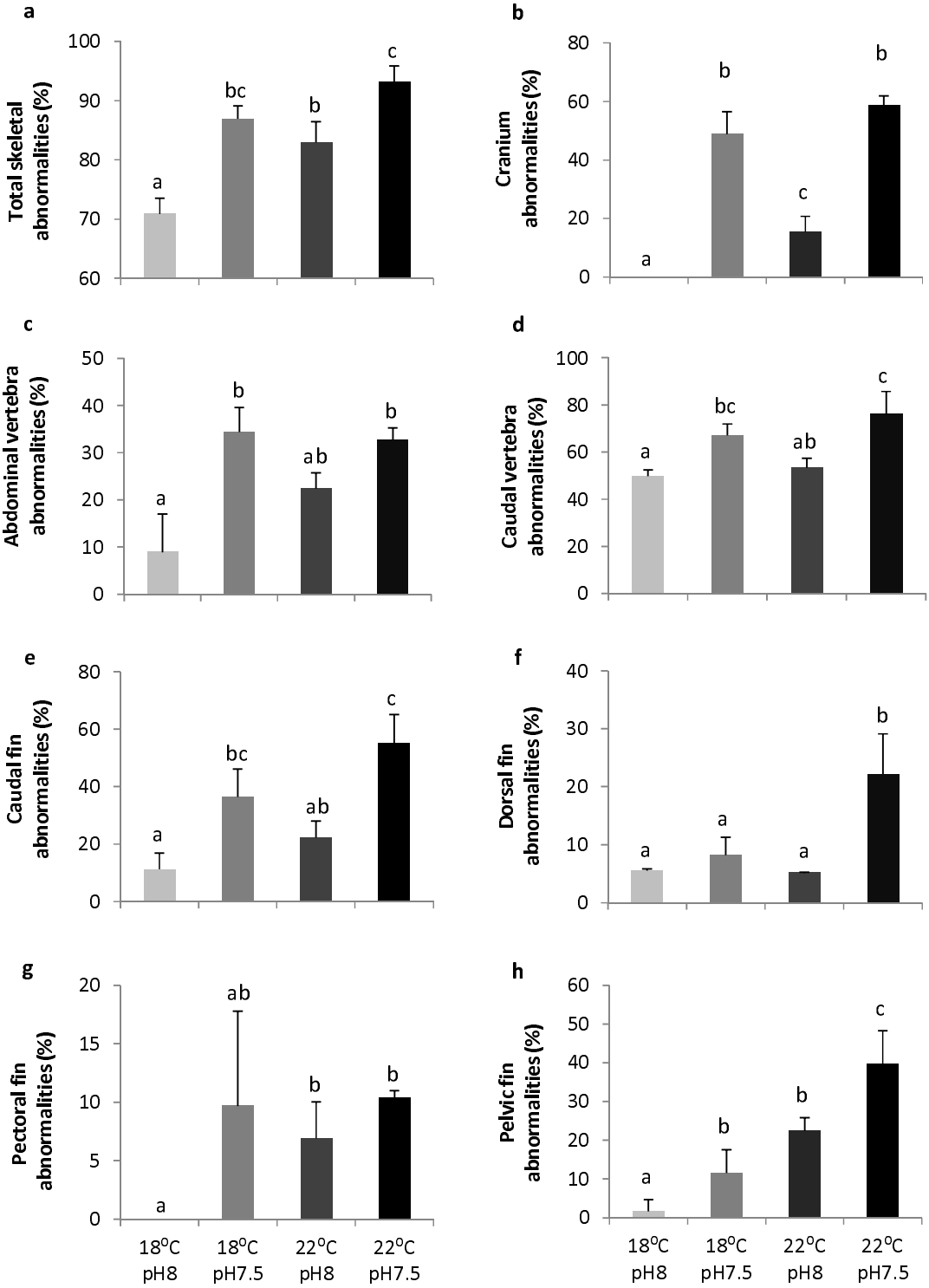

Figure 5

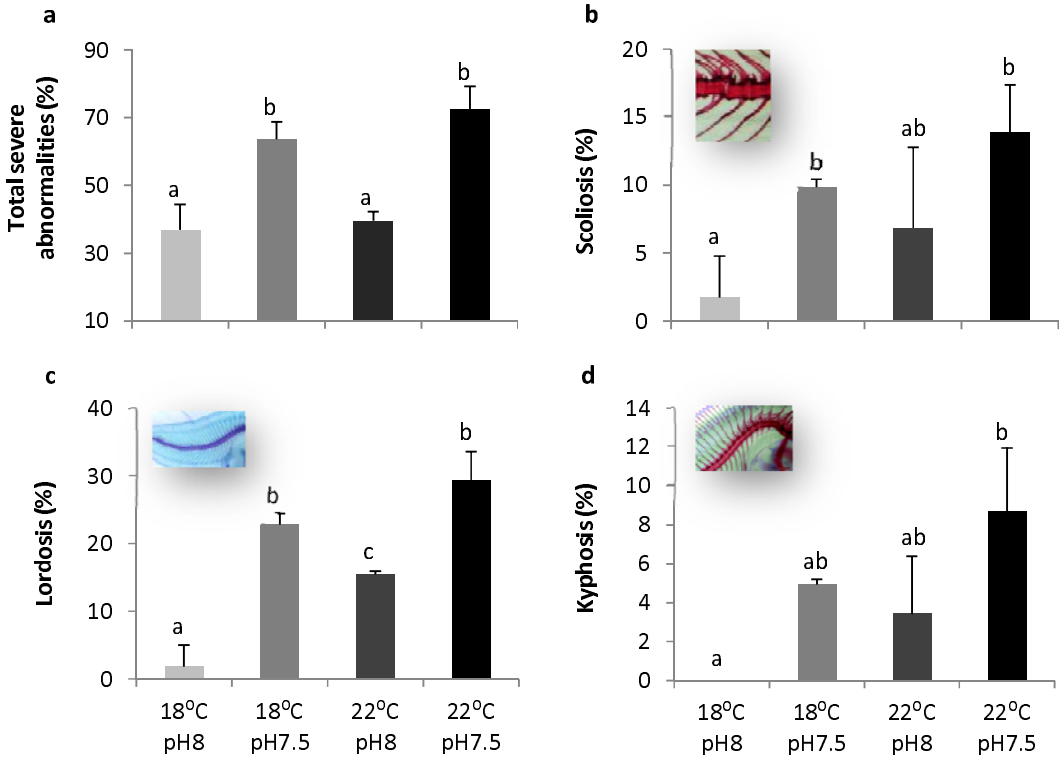

Figure 6